

Adsorption by particles injected into a gas stream

R.W.K. Allen, E.D. Archer, J.M. MacInnes*

Department of Chemical and Process Engineering, The University of Sheffield, Mappin Street, Sheffield S1 3JD, UK

Received 29 March 2000; received in revised form 4 September 2000; accepted 13 September 2000

Abstract

A theoretical model for dry sorption injection is developed. The model uses a transient diffusion equation for particles with adsorption represented using a Freundlich isotherm and a balance equation for the bulk gas phase. The case of injection of adsorbing particles having a log-normal distribution of sizes is considered. It is found that for the conditions of practical interest just three parameters determine the adsorption behaviour. These are the exponent, q , determining the non-linearity of the Freundlich equilibrium relation; the non-dimensional adsorbate capacity of the particles, $K^*\phi_T$, where K^* represents capacity per unit mass of particle and ϕ_T the mass of particles injected; and the geometric standard deviation, σ_P , of particle size in the particle population. Comparison is made between the model and existing experimental data for single particles under conditions of uniform external adsorbate concentration. The data span a range of particle geometries, sizes and adsorbate concentrations and the model is found to reproduce the entire range of data to within about $\pm 20\%$. The parameters of the model are systematically varied in a series of computations that illustrate and confirm the theoretical analyses. © 2001 Elsevier Science B.V. All rights reserved.

Keywords: Adsorption; Freundlich equilibrium relation; Dry sorption

1. Introduction

The use of particles to adsorb species in a gas has been investigated extensively in connection with applications such as gas chromatography and fixed bed adsorbers. In these applications a gas stream is passed over stationary particles which alternately adsorb and then desorb particular chemical species. In gas chromatography this allows detection of chemical species. In adsorption systems, extraction of target species is achieved. Adsorption of a significant mass of a chemical species (the adsorbate) depends on the particles (the adsorbent) having large internal surface area. Commonly, some form of activated carbon is used as the adsorbent material. Two physical processes must be represented if the adsorption rate is to be predicted: the equilibrium between the solid and gas phase concentrations of the adsorbate and the transport of adsorbate from the external gas to the interior surface of the particles. Many studies have developed models appropriate for fixed beds of particles. These have varied in complexity and include the early work by Glueckauf [4] addressing the problem of break-through curves for chromatography columns and the multi-dimensional modelling of fixed bed catalytic reactors

of Quinta Ferreira et al. [5]. The latter work includes convection of species due to flow within the bed particles. For the case of adsorption of species at low concentrations convection is not important. The work of Gray and Do and Lin et al. [1–3] uses this fact in a one-dimensional modelling approach that is demonstrated to give a good account of adsorption by single particles as well as fixed beds for small adsorbate concentration. Accurate measurement of the equilibrium curve is combined with the model to bring agreement with measurements of both adsorption and desorption rates.

Dry sorption injection, which is a method of gas cleaning based on the injection of particles into a gas stream, presents a somewhat different set of conditions than those of a fixed bed. In particle injection systems, particles travel with the gas and are smaller than is typical for fixed bed systems. Particles used in fixed beds are approximately uniform in size, typically several millimetres, while in injection systems particles have a broad distribution of size with a mean size between 10 and 100 μm . Thus, the injection systems are distinguished by the presence of a wide range of particles of smaller size as compared to those used in fixed beds, and by the fact that individual particles are free to move along with the gas.

Gray and Do [2] present a model of the adsorption process that treats the particle as having a fraction of volume occupied by microspheres that are connected by macropores leading to them from the particle exterior. The microspheres

* Corresponding author. Tel.: +44-114-222-7511;
fax: +44-114-222-7501.
E-mail address: j.m.macinnes@shef.ac.uk (J.M. MacInnes).

are the sole agent of adsorption in the model with diffusion occurring both in the macropores and in the microspheres. The model is found by Gray and Do [3] to give a reasonable account of their experimental results for SO₂ uptake by activated carbon particles. The range of conditions, however, is such that all results lie in the regime where macropore resistance to diffusion is stronger than diffusion resistance within the microspheres. The work points clearly to the need to consider the range of pore scales present in adsorbing particles and the effect these scales have on diffusion and adsorption.

The simpler modelling of Lin et al. [1] forms the basis of the work here. These authors solve the equation for time-dependent diffusion in a spherical particle of uniform porosity assuming equilibrium between gas and solid adsorbate concentration for pores at any given radial position in the particle. As in the work of Gray and Do, a Freundlich isotherm is used as the equilibrium relation. With this simple modelling as a basis, Lin et al. demonstrate good agreement with breakthrough curves in columns of activated carbon particles and fibres adsorbing benzene and vinyl chloride. The model is shown here to produce a satisfactory account of the data of Gray and Do [3].

The present work extends this previous modelling to the case of small particles possessing a distribution of sizes injected into an adsorbate-containing gas stream. Equations for the time evolution of the radial distribution of adsorbate concentration in the particles and the bulk gas adsorbate concentration are developed. Account is taken of the distribution of particle size and the example case of a log-normal distribution is considered. The model developed is solved numerically to investigate general characteristics of adsorption by particles injected into a gas stream.

2. Modelling

In dry sorption injection, particles are introduced into a gas flow and are transported with the gas as they adsorb. Here, the simplest dry sorption system is considered: injection into a uniform (plug) flow in a pipe. The depletion of adsorbate in the gas depends on the adsorbent material properties and on the gas conditions. Generally, it will be assumed that the particle properties are independent of particle size, that the gas conditions are uniform, except for adsorbate concentration, that the particles are spherical and that adsorption heating may be neglected. The latter assumption follows from restriction to low adsorbate concentration, which is the usual practical situation. Further, the physical properties of the particles and gas will be taken as constant over particle volume and throughout the gas region considered.

2.1. Particle adsorption

The conservation equation for mass fraction of an adsorbate species in the pore volume of a particle with porosity

ε may be written in terms of the gas phase density, ρ , the effective diffusivity of adsorbate in the pore gas, ϑ_e , and the mass fraction of adsorbate at radial position r in the pore gas, Y , as

$$\frac{\partial \varepsilon \rho Y}{\partial t} + \frac{1}{r^2} \frac{\partial r^2 \varepsilon \rho u_r Y}{\partial r} = \frac{1}{r^2} \frac{\partial}{\partial r} \left(r^2 \varepsilon \vartheta_e \frac{\partial \rho Y}{\partial r} \right) - \dot{m}_A \quad (1)$$

where \dot{m}_A is the rate of loss of adsorbate mass from the gas to the solid phase per unit particle volume and u_r the radial velocity of the gas in the pores. This equation expresses the balance between accumulation of adsorbate in the gas within the particle pores, the convection associated with radial gas flow caused by adsorption or desorption within the particle, the molecular diffusion of adsorbate and the mass loss to the pore walls. It is implicitly assumed that Y is an average mass fraction over all pore volume at radius r .

Eq. (1) may be simplified considerably for usual conditions of operation. First of all, the convection term is of the order of the adsorbate bulk gas mass fraction in comparison to the other terms in the equation. Thus, provided the adsorbate is present in the gas in small amounts, which is the situation of interest in dry sorption injection, the convection term is negligible and can be dropped.

The mass loss rate to the pore walls can be expressed in terms of adsorbate mass density in the pore gas, ρY , using an appropriate equilibrium relation between the adsorbed mass concentration, m , and gas concentration. The Freundlich relation is used here as it provides an adequate representation of a range of adsorbate/adsorbent systems:

$$m = K(\rho Y)^q \quad (2)$$

The solid phase concentration, m , is the adsorbed mass per unit volume of particle. When local equilibrium is assumed [1], differentiation of Eq. (2) with respect to time results in

$$\dot{m}_A = Kq(\rho Y)^{q-1} \frac{\partial \rho Y}{\partial t} \quad (3)$$

With the substitution of Eq. (3), the neglect of convection and taking the particle porosity to be uniform, Eq. (1) may be written as

$$[\varepsilon + Kq(\rho Y)^{q-1}] \frac{\partial \rho Y}{\partial t} = \frac{1}{r^2} \frac{\partial}{\partial r} \left(r^2 \varepsilon \vartheta_e \frac{\partial \rho Y}{\partial r} \right) \quad (4)$$

This equation may be solved for adsorbate mass fraction as a function of time and radial position in the particle once appropriate boundary conditions are supplied.

The boundary condition at the particle centre results from symmetry. At the outer boundary one could solve the time-dependent diffusion equation in the external gas region surrounding the particle. The time scale for change in the outer solution for concentration is D_p^2/ϑ , where D_p is the particle diameter and ϑ the free gas diffusivity of adsorbate. The time scale for change in conditions within the particle depends (Eq. (4)) not only on diffusion but also on adsorption of gas molecules onto pore surfaces. As has been

pointed out by Lin et al. [1], the second of the two terms in the square brackets on the right-hand side is dominant since the mass per volume of adsorbate in the solid phase at equilibrium exceeds that in the gas phase for the large surface area per volume in the particles of interest. One can see from Eq. (4) that the diffusion in a particle with adsorption taking place is approximately the same as for pure diffusion in a particle with the equivalent diffusivity of $\varepsilon \vartheta_e (\rho Y)^{1-q} / Kq$. This allows the ratio of the time scales of changes in the external and internal conditions to be approximated as

$$\frac{1}{q} \frac{\vartheta_e}{\vartheta} \left[\frac{\rho \varepsilon Y}{K(\rho Y)^q} \right]$$

The quantity in square brackets is the ratio of adsorbate mass in the gas and adsorbate mass in the solid within the particle. With q of order unity, the ratio of effective and free gas diffusivities smaller than unity and the gas–solid mass ratio much less than unity, one can conclude that the time scale characterising external changes is much smaller than that characterising internal changes. As a result, the external conditions may be taken as approximately steady and a simple mass transfer coefficient, h , at the particle surface can be used to express the exterior mass exchange with the bulk gas. The boundary conditions for Eq. (4) are then

$$\begin{aligned} \varepsilon \vartheta_e \frac{\partial \rho Y}{\partial r} &= \rho h (Y_B - Y_S) \\ \text{at } r &= \frac{D_P}{2} \text{ and } \frac{\partial Y}{\partial r} = 0 \text{ at } r = 0 \end{aligned} \quad (5)$$

The mass fractions Y_B and Y_S in the first relation are evaluated in the bulk gas far from the particle and at the particle surface, respectively. The mass transfer coefficient is obtained here in terms of Reynolds number, Re , and Schmidt number, Sc , [6] using

$$\begin{aligned} h &= \frac{\vartheta}{D_P} (2 + 0.6 Re^{1/2} Sc^{1/3}), \\ Re &= \frac{\rho |u_P - U| D_P}{\mu}, \quad Sc = \frac{\mu}{\rho \vartheta} \end{aligned} \quad (6)$$

In these relations, U is the velocity in the gas in the vicinity of the particle, u_P the particle velocity, and ρ and μ are the density and viscosity of the gas.

From Eqs. (1)–(5) it can be seen that the adsorption process for a single particle in the gas flow depends on a large number of properties of the particle and the gas, as well as on flow conditions. A considerably simpler view arises from an appropriate non-dimensionalisation of the equations. Defining non-dimensional variables

$$\begin{aligned} Y^* &= \frac{Y}{Y_{B_0}}, \quad t^* = \frac{t \vartheta_e}{D_P^2 (1 + K^*)}, \\ r^* &= \frac{r}{D_P}, \quad K^* = \frac{Kq(\rho Y_{B_0})^{q-1}}{\varepsilon} \end{aligned} \quad (7)$$

involving the initial bulk gas mass fraction of adsorbate, Y_{B_0} , and the gas and particle properties, Eq. (4) becomes

$$\left[\frac{1 + K^*(Y^*)^{q-1}}{1 + K^*} \right] \frac{\partial Y^*}{\partial t^*} = \frac{1}{r^{*2}} \frac{\partial}{\partial r^*} \left(r^{*2} \frac{\partial Y^*}{\partial r^*} \right) \quad (8)$$

subject to the boundary conditions,

$$\frac{\partial Y^*}{\partial r^*} = \begin{cases} Bi(Y_B^* - Y_S^*), & r^* = \frac{1}{2} \\ 0, & r^* = 0 \end{cases} \quad (9)$$

Non-dimensionalisation of the boundary conditions has resulted in the appearance of the Biot number,

$$Bi = \frac{h D_P}{\varepsilon \vartheta_e} \quad (10)$$

It can be noted that the time scale used to non-dimensionalise time (that used also in [1]) in the second of Eq. (7) is consistent with the time scale resulting from the idea of an equivalent diffusivity mentioned earlier.

One can see from the non-dimensional form of the equations that the solution, in terms of non-dimensional quantities, depends on only four parameters: the non-dimensional adsorption parameter, K^* , the Freundlich exponent, q , the Reynolds number, Re , and the Schmidt number, Sc . This in itself is a considerable simplification when setting out to understand the particle diffusion and adsorption process in dry sorption injection. However, if one considers that the effective diffusivity within the pores of a particle is considerably less than the diffusivity in the exterior gas (a result of Knudsen effects and the tortuous path along which diffusion occurs), then considerable further simplification is possible. The greater exterior diffusivity results in a large Biot number, which in turn means that mass transfer is controlled by the rate of diffusion into the particle interior and not by that from the bulk gas to the particle surface. From the first condition of Eq. (9), one finds, since $\partial Y^* / \partial r^* = O(1/\sqrt{t^*})$ at the particle surface, that $Y_S^* = Y_B^*$ provided $Bi\sqrt{t^*} \gg 1$. Thus, for large Biot number the external transfer has negligible effect on adsorption. An exception to this is the adsorption at very early times, where t^* is small. Typically, the ratio of external to internal diffusivity is 10 or greater and $\varepsilon \approx 0.5$, so from Eqs. (6) and (10), $Bi > 40$. For $Bi = 40$, external diffusion will thus have a strong effect only at non-dimensional times less than around $t^* = 0.0006$. The present results show that little adsorption occurs at such early times (Fig. 3). Thus, the Biot number does not influence the solution significantly and one can conclude that the diffusion and adsorption of adsorbate within the particle does not depend strongly on the conditions of the outer gas flow, i.e. does not depend strongly on the Reynolds and Schmidt numbers. Exceptions to these conclusions would arise only for particles having extremely large and straight pores where the Knudsen effects and tortuosity were small.

Further simplification is possible as a result of the fact that high mass concentration is invariably associated with adsorbate in the condensed phase as compared with the gas

phase, as mentioned previously. This means that the parameter K^* will be large, and from Eq. (8), one can see that as $K^* \rightarrow \infty$ it no longer affects the solution. (This simplification also is implicit in the formulation of Lin et al. [1].) For particles of practical interest, then, one concludes that the process of diffusion into the particles is governed by just one non-dimensional parameter: the Freundlich exponent, q . Of course, additional parameters enter the problem through the equations governing particle motion, which determines the position of particles in the flow, and change in bulk adsorbate concentration in the gas.

2.2. Particle motion

Adsorption by the particles may depend on the gas motion. As a simple test flow, the case of particles introduced into a plug pipe flow at velocity U in the vertical direction is considered. Vertical flow allows the assessment of holdup effects on adsorption. The particles are introduced from rest and allowed to accelerate under the influence of drag and gravity. The equation for change in particle velocity when particle density (ρ_P) is much greater than the gas density may be written (e.g. [7]) as

$$\frac{du_P}{dt} = -g - \frac{(u_P - U)}{\tau_S} \left[1 + \frac{Re^{2/3}}{6} \right] \quad (11)$$

where τ_S is the Stokes time scale:

$$\tau_S = \frac{\rho_P D_P^2}{18\mu} \quad (12)$$

The time taken to reach the terminal velocity, having been released from rest, is related to the Stokes time scale and so the proportion of the adsorption process during which the particle accelerates to the terminal velocity is related to the ratio of the Stokes time scale and the particle diffusion time scale, τ_A (implicit in t^* of Eq. (7)):

$$\frac{\tau_S}{\tau_A} \propto \left(\frac{\rho_P}{\rho} \right) \left(\frac{1}{1 + K^*} \right) \left(\frac{\rho \vartheta_c}{\mu} \right) \quad (13)$$

As mentioned previously, $K^* \gg 1$ and the effective diffusivity of gas in the particle pores is smaller than the diffusivity in free gas. This means that the product of the second and third factors on the right-hand side of (13) is small. The density ratio factor, on the other hand, is large. However, it appears likely that the small magnitudes of the second and third factors dominate the overall product of the right-hand side and the Stokes time scale is much smaller than the diffusion time scale. In this case, the time taken for the particles to accelerate to the terminal velocity is negligible in comparison to the time taken for the adsorption process. This means that one could ignore the brief period of acceleration and simply represent the particle movement as constant and equal to the terminal velocity. (In the computations presented, Eq. (11) is solved and the acceleration time confirmed to be unimportant for the range of conditions considered.)

2.3. Adsorbate uptake

The loss of adsorbate from the bulk gas flow depends on uptake by the particles. This uptake depends in turn on the distribution of particle sizes in the population of injected adsorbent particles. For particles with a size distribution $f_V(D_P)$, defined as the differential volume fraction of particles per differential particle diameter at size D_P , the balance on adsorbate mass in the bulk gas is expressed as

$$\frac{d\rho U Y_B}{dx} = - \int_0^\infty \dot{m} \frac{\phi}{V_P} f_V dD_P \quad (14)$$

where Y_B is the mass fraction of adsorbate in the bulk gas, x the distance along the pipe, ϕ the total particle volume fraction in the flow at x , \dot{m} the instantaneous adsorbate mass transfer rate to a single particle of size D_P , and V_P the volume of a particle of size D_P . The integral on the right-hand side of the equation is over all particle diameters at position x and gives the total rate of adsorbate mass transfer per volume.

It is helpful to non-dimensionalise Eq. (14) to discover what additional parameters enter the problem in connection with the decreasing level of adsorbate concentration in the bulk gas. With length scaled using the particle adsorption time and the gas bulk velocity, one finds that

$$\frac{dY_B^*}{dx^*} = - \frac{6}{\pi} (1 + K^*) \phi_T \phi^* \int_0^\infty \dot{m}^* \frac{f_V^*}{(D_P^*)^3} dD_P^* \quad (15)$$

where the new non-dimensional quantities appearing are defined as follows:

$$x^* = \frac{x \vartheta_c}{U \bar{D}_P^2} \frac{1}{1 + K^*}, \quad \phi^* = \frac{\phi}{\phi_T}, \quad \dot{m}^* = \frac{\dot{m}}{\rho \bar{D}_P Y_{B_0} \vartheta_c},$$

$$f_V^* = f_V \bar{D}_P, \quad D_P^* = \frac{D_P}{\bar{D}_P} \quad (16)$$

The volume fraction has been normalised using the value of volume fraction, ϕ_T , prevailing once all particles have reached the terminal velocity. This volume fraction will be defined below. A mean diameter of the particle distribution, \bar{D}_P , has been used as a characteristic scale of particle size in these relations. This is a reminder that the particle equations contain a range of time and length scales associated with the distribution of particle size. The mean diameter of the distribution is just one of the parameters required to specify completely the distribution of scales. The higher moments of the distribution must be included as additional parameters.

In the present work, a log-normal distribution will be assumed:

$$d\varphi = \frac{1}{\sqrt{2\pi}} \exp \left\{ -\frac{\xi^2}{2} \right\} d\xi \quad (17)$$

where φ is the volume fraction of particles in $d\xi$ at ξ , with ξ the normalised diameter

$$\xi = \frac{\ln(D_P/\bar{D}_P)}{\ln \sigma_P} \quad (18)$$

The distribution used here, then, is specified in terms of just two parameters: the geometric mean particle size, \bar{D}_P , and the geometric standard deviation, σ_P . Thus, the geometric standard deviation enters as a further non-dimensional parameter affecting the adsorption.

Solution of Eq. (14) requires ϕ to be determined. The conservation of mass of particles of size D_P in size interval dD_P in the flow requires that

$$\phi f_V dD_P = \frac{\dot{M}}{\rho_P A u_P} f_{V_0} dD_P \quad (19)$$

In this relation, \dot{M} is the total particle mass flow rate, A the cross-sectional area of the pipe and f_{V_0} the distribution function at injection. The distribution function changes with x because particles of different size accelerate at different rates and reach different terminal velocities and, hence, each particle size has a different velocity function with x . The distribution function and particle volume fraction, ϕ , at any x position is determined by Eq. (19), which gives $\phi f_V dD_P$ in terms of known quantities, and the fact that the integral of the distribution function over all particle sizes is unity. In particular, the value ϕ_T , the particle volume fraction when all particle sizes have reached mean equilibrium motion in the gas flow, is given by

$$\phi_T = \frac{\dot{M}}{\rho_P A} \int_0^\infty \frac{1}{u_{PT}} f_{V_0} dD_P \quad (20)$$

where u_{PT} is the terminal velocity of particles of size D_P in gas at velocity U .

The further non-dimensional parameters introduced by the interaction of the particles with the bulk gas can now be seen. With a uniform bulk gas concentration, the Freundlich exponent, q , is the single parameter governing the adsorption when K^* is large. A depleting bulk concentration introduces the parameters K^* , ϕ_T and σ_P . The first of these additional parameters represents the capacity of the particles to hold adsorbate and the second the mass rate of particles. For large K^* , one can see from Eq. (15) that the effects of capacity and particle mass rate are indistinguishable and the two parameters K^* and ϕ_T can be replaced by the single parameter $K^* \phi_T$. Thus, dry sorption injection under the practical conditions laid out in the above modelling depends on just three non-dimensional parameters: the equilibrium exponent, q , the particle capacity $K^* \phi_T$, and for a log-normal particle size distribution, the geometric standard deviation, σ_P .

2.4. Numerical approach

The equations are solved using a fully explicit finite volume approach in which the radial direction in the equations for particle adsorption are divided into 60 uniformly spaced grid cells. Particle diameter space has been divided into 25 grid cells. Thus, 25 sets of the discrete particle equations are solved together with the equation for bulk adsorbate mass fraction. Each of the 25 sets of particle equations

corresponds to a discrete range in particle diameter space, ΔD_P , contributing a partial volume fraction of $\phi f_V \Delta D_P$ to the total particle volume fraction in the gas flow. The bulk mass fraction equation is integrated along the x direction, with the particle equations being integrated in time up to the end of each successive spatial step in the x direction. The spatial step, Δx , is chosen such that the time interval for the smallest discrete particle to traverse that distance is

$$\Delta t = 10 \frac{(\Delta r)^2}{\vartheta_e} (1 + K^*) \quad (21)$$

where Δr is the radial size of the grid cells. This choice of time step size ensures that for all particle sizes in the population the time step is much less than the time scale for changes in the particle conditions. Further refinement in either time or radial resolution changed the solution by less than 1%.

3. Results

Computations have been made for a wide range of the non-dimensional parameter values. The actual physical parameters used in the computations are given in Table 1. The basic conditions considered correspond to adsorbate in an air stream at atmospheric pressure around 160°C, with a bulk gas velocity of 10 m/s. For purposes of specifying the gas mass flow rate and, hence, establishing a reference for particle mass flow rate, the pipe diameter is taken to be 0.1 m. The non-dimensional parameters are varied by changing the equilibrium coefficient and exponent, the mass flow rate of particles, the particle mean size and standard deviation.

3.1. Constant bulk gas concentration

As particle mass flow rate, \dot{M} , approaches zero, the adsorbate loss from the bulk gas becomes negligible and the bulk gas mass fraction remains fixed. For this condition, the solution should depend only on the Freundlich exponent, q . This indeed is found to be the case. Computations with a range of K values showed that the results plotted in terms of the non-dimensional variables collapsed to a single curve for a given value of q . Fig. 1 shows radial profiles of adsorbate mass fraction plotted at a number of non-dimensional

Table 1
Conditions used in the computations

Gas properties	Particle properties
ρ : 0.9 kg/m ³	ρ_P : 1000 kg/m ³
μ : 2×10^{-5} Pa s	ε : 0.5
ϑ : 10^{-5} m ² /s	ϑ_e : 10^{-7} m ² /s
	K : $1-10^7$ (units depending on q)
Flow	q : 0.3–1.0
U : 10 m/s (also 0.187–10 m/s)	\bar{D}_P : 5–80 μ m
\dot{M} : 0.001–0.64 kg/s (ϕ_T : 1.2×10^{-5} – 4.0×10^{-4})	σ_P : 1.0–3.0

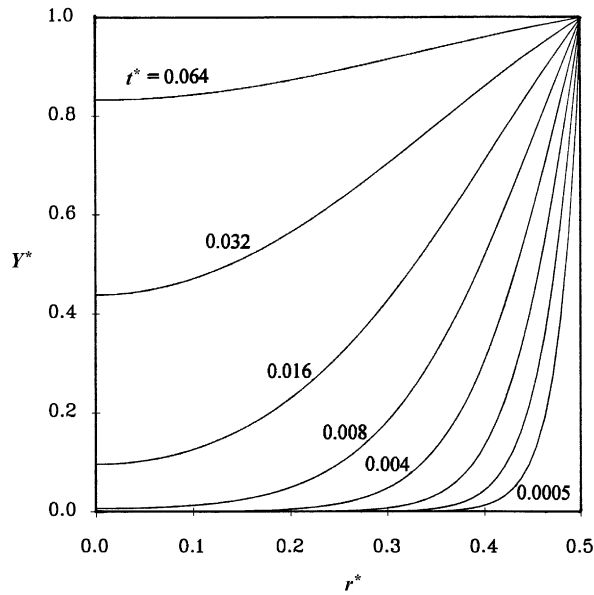


Fig. 1. Radial profiles of gas adsorbate mass fraction within the particle at a series of times during the adsorption process. The bulk gas mass fraction is constant in time and $m = 3 \times 10^5 \rho Y$.

times throughout the adsorption process for the case of a linear equilibrium relation ($q = 1.0$). Since the Biot number is large and the bulk concentration is fixed, the mass fraction at the outer surface of the particle remains near unity. The progression of a diffusion wave into the centre of the particle may be seen in the figure. In Fig. 2, the effect of a fractional equilibrium exponent (in this case $q = 0.3$) can be seen. The leading edge of the diffusion wave is made steeper, reflecting the relatively greater adsorption at small concentration as q is decreased, and the progression of the

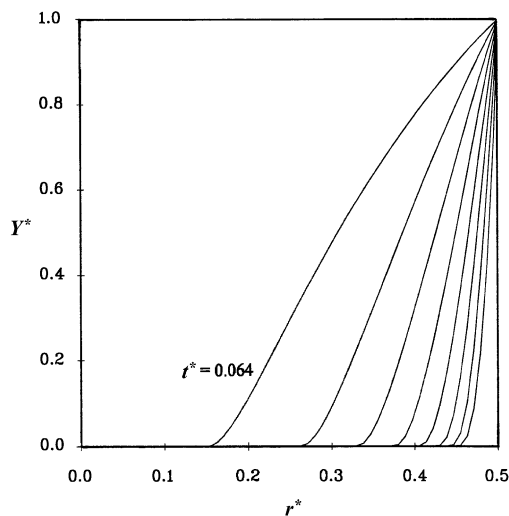


Fig. 2. Radial profiles of gas adsorbate mass fraction within the particle at a series of times during the adsorption process. The bulk gas mass fraction is constant in time and $m = 3 \times 10^5 (\rho Y)^{0.3}$. Profiles plotted at the same non-dimensional times as in Fig. 1.

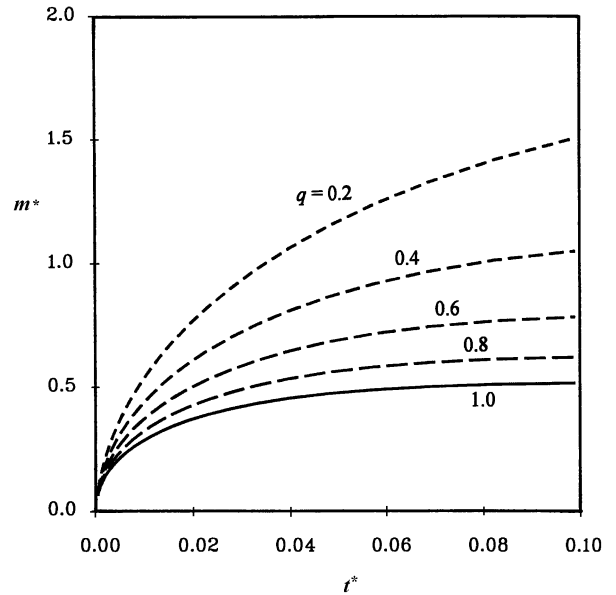


Fig. 3. Effect of Freundlich isotherm exponent, q , on the non-dimensional adsorbed mass in a particle at fixed K ($m = 3 \times 10^5 (\rho Y)^q$).

adsorbate into the centre of the particle is much slower in terms of the non-dimensional time.

The effect of q on adsorption may be illustrated by plotting the adsorbed mass in the particle as a function of time. Fig. 3 shows the results plotted with non-dimensional variables for different values of q and fixed K . The non-dimensional adsorbed mass is

$$m^* = \int_0^{t^*} \dot{m}^* dt^* = \frac{1}{\rho D_p^3 \varepsilon Y_{B_0} (1 + K^*)} \int_0^t \dot{m} dt \quad (22)$$

It can be seen in the figure that when q is small, adsorption remains more rapid at longer non-dimensional times than for large q . This is a result of the increasing adsorbed mass capacity with decreasing q and fixed K .

Gray and Do [3] measured adsorbed mass of sulphur dioxide for activated carbon particles formed into spheres, cylinders and slabs. The effect of bulk gas variation caused by adsorption was reduced by supplying the adsorbate gas mixture, sulphur dioxide and helium, at high flow rate. Results for the fraction of equilibrium SO_2 mass adsorbed by the particle with time are reported for the different particle geometries and for various particle sizes and SO_2 bulk concentrations. As expected, the Biot number is large for all cases reported. The present model may be adapted in a straightforward manner to the various geometries. Taking K^* to be large, Eq. (8) may be generalised for these geometries to the form

$$Y^{*q-1} \frac{\partial Y^*}{\partial t^*} = \frac{1}{r^{*m}} \frac{\partial}{\partial r^*} \left(r^{*m} \frac{\partial Y^*}{\partial r^*} \right)$$

where $m = 0, 1$ or 2 for the linear, cylindrical and spherical geometries, respectively. The Biot number is greater than 30 for all the experimental cases and so the outer boundary

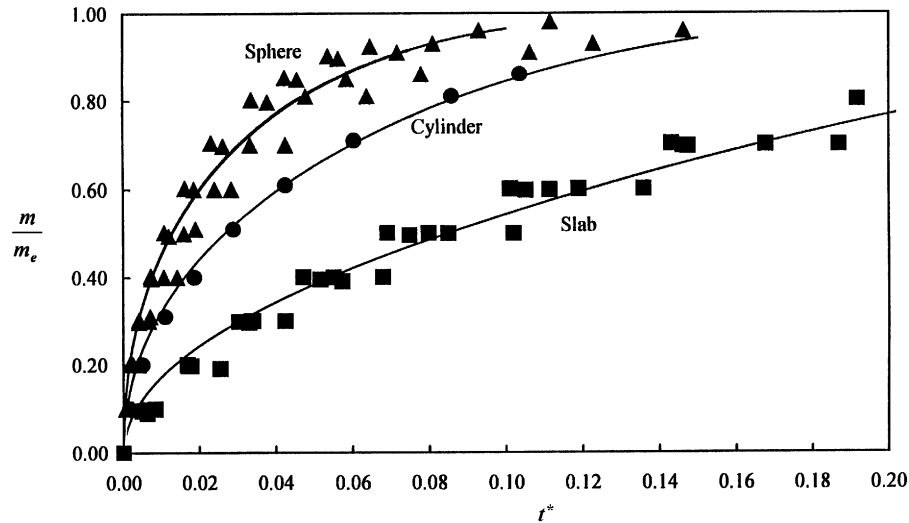


Fig. 4. Comparison of the model with the experimental results of Gray and Do [3]. Symbols, experiment; curves, model with $q = 0.461$.

condition $Y_S^* = Y_B^*$ is used. The non-dimensional quantities are as before (Eq. (7)), as is the dependence on a single non-dimensional parameter q (since bulk concentration in each experiment should remain constant). This equilibrium parameter was determined by Gray and Do to be 0.461 by fitting the range of experimental results. In other words, the equilibrium characteristics of the particles were taken as being independent of particle geometry. In this case, all of the experimental results should collapse to just three universal curves according to the present model, one for each of the three geometries.

Fig. 4 shows the data plotted in terms of the non-dimensional parameters of the model with the three model curves. The collapse of the data is evident, although the results scatter about the model curves in a band of results deviating from the model by around $\pm 20\%$. The authors note a concern about the adequacy of the supply rate of fresh mixture for conditions of rapid adsorption, leading to a reduction in effective bulk concentration. Lowering the bulk concentration of SO_2 would result for such cases in a lower mass uptake rate than expected. The cases with smaller particle size (D_p) and larger Y_{B_0} give relatively rapid adsorption according to the model (Eq. (7)). The shift in uptake curves to the right in the data for a given geometry is associated with both decreasing size and increasing SO_2 concentration. Thus, it is possible that at least part of the scatter is due to changing experimental conditions that were not measured. In any case, the present model clearly gives a reasonable account of the particle uptake and for the range of particle geometry of the experiments.

3.2. Varying bulk gas concentration

Introducing significant particle mass flow produces changing bulk adsorbate mass fraction and the effect on

the particle adsorption is large. Fig. 5 shows the effect of increasing particle mass flow rate to 0.008 kg/s, corresponding to a particle volume fraction of 10^{-4} for the gas flow rate conditions used (Table 1) and with $K = 10^4$, $q = 1.0$, $\bar{D}_p = 10 \mu\text{m}$ and $\sigma_p = 1.0$ (i.e. particles of uniform size). The non-dimensional times plotted are the same as before. The falling value of bulk mass fraction is evident in the dropping mass fraction at the particle surface and the particle reaches saturation somewhat sooner than before. The effect of the parameter ϕ_T is shown in Fig. 6, where

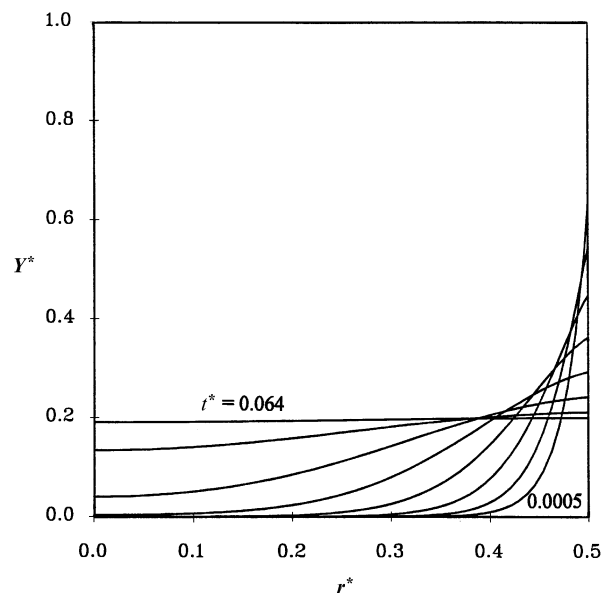


Fig. 5. Effect of non-uniform bulk concentration. Radial profiles of gas adsorbate mass fraction within the particle at a series of times during the adsorption process. The bulk gas mass fraction is constant in time and $m = 10^4 \rho Y$, $D_p = 10 \mu\text{m}$, $\phi_T = 4 \times 10^{-4}$. Profiles plotted at the same non-dimensional times as in Fig. 1.

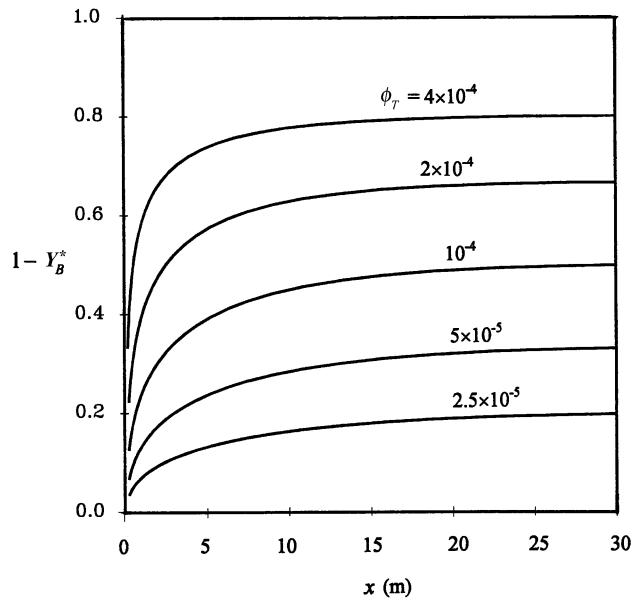


Fig. 6. Effect of non-dimensional particle mass injection rate, ϕ_T , on adsorbate uptake ($m = 10^4 \rho Y$ and $D_p = 10 \mu\text{m}$).

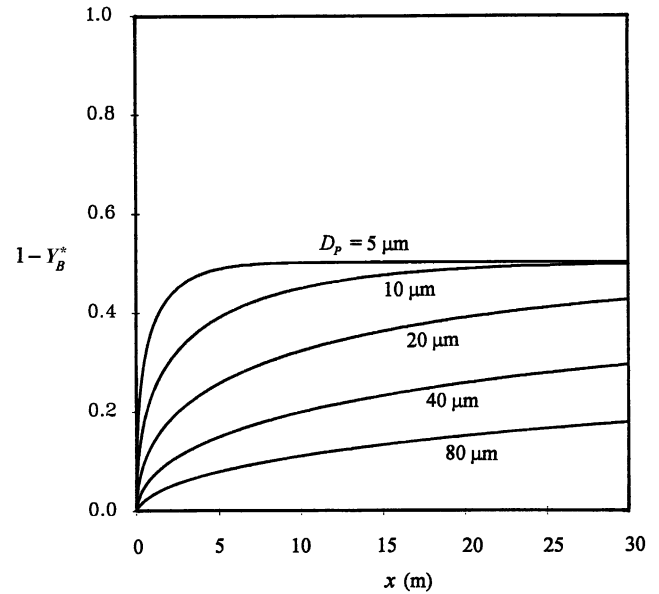


Fig. 7. Effect of particle size on adsorbate uptake ($m = 10^4 \rho Y$ and $\phi_T = 10^{-4}$).

results are shown of computations as above but with a range of particle mass flow rates. The figure shows the fraction of adsorbate adsorbed from the gas (uptake) as a function of distance along the pipe. The effect of increasing particle mass flow rate is to increase the adsorption capacity, thereby decreasing the equilibrium gas concentration and increasing the uptake. The plot is against dimensional distance downstream. Re-plotting the results in terms of x^* would not alter the plot except to change the scale on the horizontal axis.

Varying the particle diameter for the conditions of the previous paragraph, again with a particle mass flow rate of 0.008 kg/s , results in the expected slower rate of adsorption with increasing particle size as shown in Fig. 7. Here, the curves should come closer together when plotted with respect to non-dimensional distance, x^* . Indeed, when this was done, the results collapsed to a single curve indicating that acceleration effects are negligible. If acceleration was significant, the larger particles would take longer time to travel down the pipe than the smaller ones and would have a steeper initial slope in the non-dimensional uptake curve.

Under conditions of low gas stream velocity, the particle terminal velocity can approach zero and the residence time in a given length of pipe can increase significantly. Computations were made for a range of gas velocities, maintaining the gas flow rate constant by increasing the pipe diameter as the gas velocity was reduced. An $80 \mu\text{m}$ particle was considered, for which the terminal velocity relative to the gas is 0.156 m/s , according to the model. The results for gas velocities between 0.187 (just 20% greater than the terminal particle velocity) and 2.49 m/s are plotted in Fig. 8. A clear effect is seen although only at gas velocities less than about four times the velocity at which the particle would

remain fixed (theoretically) in position in the pipe. (In practice, of course, such particles may be able to drop down in the pipe due to regions of lower gas velocity near the pipe walls which is ignored in the computations here.) The effect found is due only to the reduced rate that particles are carried up the pipe and not to increased external mass transfer rates, i.e. the Reynolds number effects in Eq. (6). When the results were re-plotted using non-dimensional time for

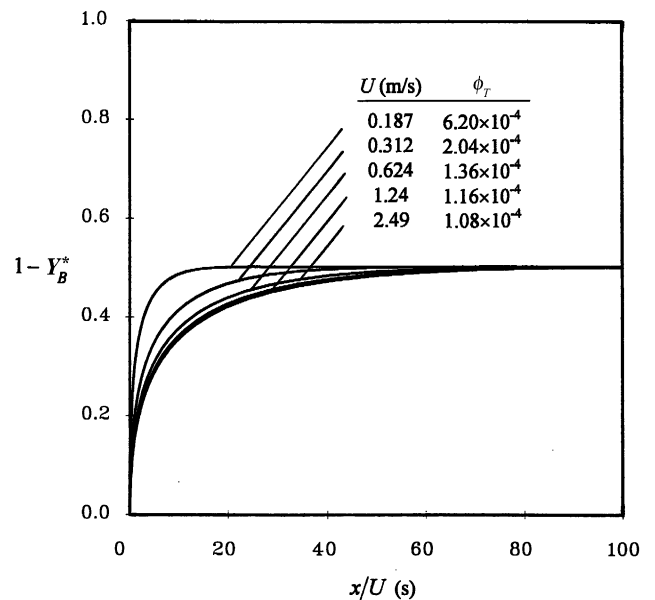


Fig. 8. Uptake as the gas velocity approaches the particle terminal velocity. $m = 10^4 \rho Y$, $D_p = 80 \mu\text{m}$, $\phi_T = 10^{-4}$ for large U . Terminal velocity of particles is 0.156 m/s .

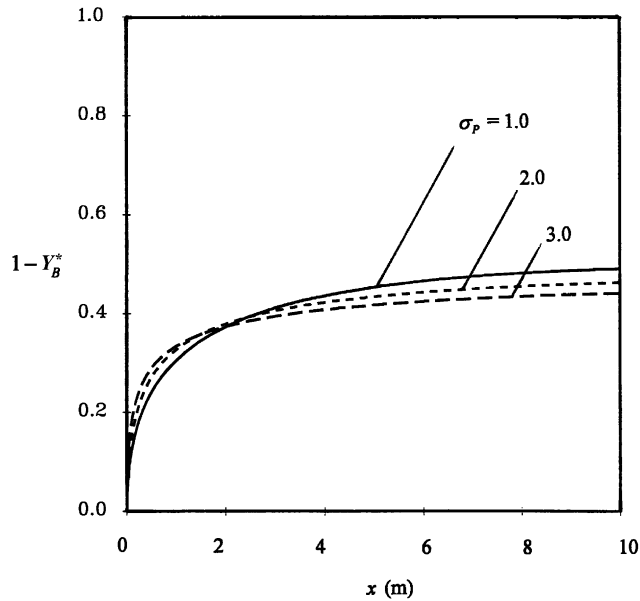


Fig. 9. Influence of standard deviation of particle size distribution on uptake ($m = 10^4 \rho Y$, $D_p = 10 \mu\text{m}$, $\phi_T = 10^{-4}$).

the horizontal axis in place of non-dimensional distance, the results collapsed quite precisely to a single curve. The effect of the particle ‘holdup’ at these low gas velocities is seen also in the terminal value of particle volume fraction in the flow. These values are listed in the figure and indicate a rise in the particle volume fraction by about a factor of 6 in the case of the smallest gas velocity shown.

Finally, the effect of particle size distribution is examined. Clearly, smaller particles in the population will become saturated most rapidly, while larger particles will saturate least rapidly. Computations are shown in Fig. 9 of the uptake produced with a $10 \mu\text{m}$ particle mean size and particle size log-normally distributed with standard deviations of 1.0, 2.0 and 3.0. One can see the uptake initially increasing with increasing standard deviation as more smaller particles are introduced. Later in the uptake process, the broader distribution results in a reduction in the uptake rate. Eventually, all three uptake curves must reach the same asymptotic value since the particle properties and particle mass rates are the same. The broader distribution of size for fixed mean size gives not only more smaller particles but also more larger particles and at later times the longer time scale of the larger particles characterises the adsorption rate. At intermediate times, the smaller particles come into approximate equilibrium with the bulk gas having taken up only a portion of the ultimate capacity of the particles. Then as larger particles continue to reduce the bulk concentration, the smaller particles begin desorbing to come into equilibrium with the changing bulk gas composition. This is shown in Fig. 10 by a plot of non-dimensional adsorption rate associated with particles of different size for the case of a standard deviation of 2.0.

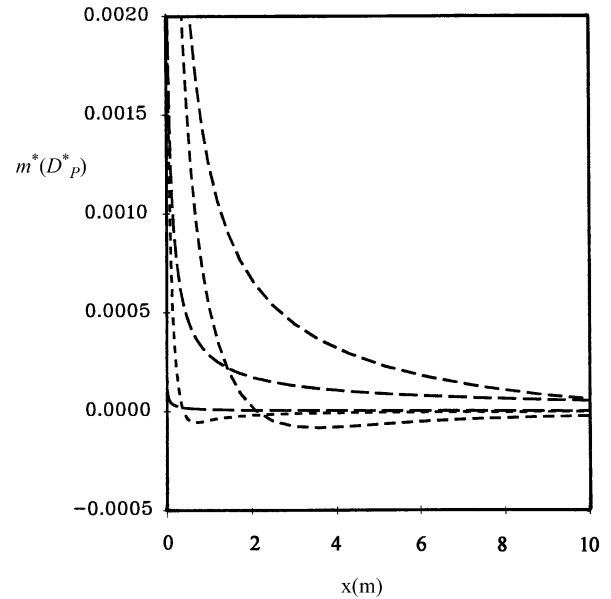


Fig. 10. Non-dimensional mass adsorption rates for particles of different size in the computation of Fig. 9. $D_p = 1.7, 4.1, 10.0, 24.0$ and $59.0 \mu\text{m}$, length of dashed line increasing with particle size.

4. Conclusion

A theoretical model for dry sorption injection, i.e. the adsorption by small particles injected into a gas stream, has been developed and analysed. The approach uses solution of a one-dimensional transient diffusion equation with adsorption to compute the time-dependent radial distribution of adsorbate mass fraction in the particle pores. Injection into the gas flow upwards in a vertical plug flow in a pipe is considered with particle properties taken as uniform. For purposes of the analysis and computations, equilibrium is represented using a Freundlich isotherm and a log-normal distribution of particle sizes is used.

A surprisingly simple picture of the adsorption process emerges from the analysis. A number of simplifications may be made to the general formulation for the conditions of interest. These simplifications result from the greater gas diffusivity within the pores than in the external gas, the small adsorbate concentrations of interest and the small mass of adsorbate in the gas phase within the particle as compared to that in the solid phase. For the Freundlich isotherm and log-normal particle size distribution used in the model computations, it is shown that, with the stated restrictions, the adsorption process of practical interest in dry sorption injection depends on just three non-dimensional parameters: q , $K^* \phi_T$ and σ_p . The exponent, q , in the Freundlich equilibrium relation determines the relative importance of adsorption as the bulk gas adsorbate composition varies during uptake. The second parameter is the non-dimensional product of equilibrium coefficient and particle mass injection rate, $K^* \phi_T$, and represents the equilibrium capacity of the particles to

hold the adsorbate. The final parameter is the geometric standard deviation, σ_P , of the log-normal size distribution.

As a result of the relatively small diffusivity for gas within the particles in dry sorption injection, the effect of the external flow and transfer is not significant and the adsorption process is found to be insensitive to both the Reynolds and the Schmidt numbers. The results have suggested, in fact, that the only effect due to flow comes through alteration of the particle residence time. When gas velocities nearing the particle terminal velocity were used, the more rapid uptake with distance along the flow was shown to be purely due to increased time in the gas, even for relatively large particle size.

From a practical point of view, the scaling of the adsorption time is revealing and the effect of size distribution is noteworthy. The process of adsorption has been shown to proceed with the characteristic time implicit in the second of Eq. (7). That is, adsorption time is proportional to the square of particle diameter and the characteristic equilibrium capacity of the particle, and is inversely proportional to the pore diffusivity. Thus, decreasing particle size, decreasing particle capacity and increasing pore diffusivity each serve to speed up the adsorption process. The particle size distribution further modifies the adsorption performance. A broader distribution of size has been shown to produce a more rapid initial uptake rate but a less rapid later uptake

rate as compared to that expected for particles of the mean size. This means that broadening the size distribution while maintaining a fixed mean size leads to more rapid uptake but only partial use of the total particle capacity.

References

- [1] T.-F. Lin, J.C. Little, W.W. Nazaroff, Transport and sorption of organic gases in activated carbon, *J. Environ. Eng.* (March 1996) 169–175.
- [2] P.G. Gray, D.D. Do, Adsorption and desorption of gaseous sorbates on a bidispersed particle with Freundlich isotherm. I. Theoretical analysis, *Gas Separation Purification* 3 (1989) 193–200.
- [3] P.G. Gray, D.D. Do, Adsorption and desorption of gaseous sorbates on a bidispersed particle with Freundlich isotherm. II. Experimental study of sulphur dioxide sorption on activated carbon particles, *Gas Separation Purification* 3 (1989) 201–208.
- [4] E. Glueckauf, Formulae for diffusion into spheres and their application to chromatography Theory of Chromatography, *Transactions of the Faraday Society*, Part 10 51 (1955) 1540–1551.
- [5] R.M. Quinta Ferreira, A.C. Costa, A.E. Rodrigues, Dynamic behaviour of fixed-bed reactors with large-pore catalysts: a bi-dimensional heterogeneous diffusion/convection model, *Comp. Chem. Eng.* 16 (1992) 721–751.
- [6] P.N. Rowe, K.T. Claxton, J.B. Lewis, Heat and mass transfer from a single sphere in an extensive flowing fluid, *Trans. Inst. Chem. Engrs* 41 (1965) T14.
- [7] R. Clift, J.R. Grace, M.E. Weber, *Bubbles, Drops, and Particles*, Academic Press, New York, 1978.